

Effect of temperature in bands structure, effective mass and correlation with magneto- transport properties in a nanostructure far-infrared detector superlattice

A. IDBAHA^a, A. NAFIDI^{a*}, K. KHALLOUQ^a, H. CHARIFI^a, H. CHAIB^a, B. M. SOUCASE^b,
M. A. MOLLAR GARCÍA^b, K. CHANDER SINGH^c, A. KHALAL^a, M. MASSAQ^a,
T. EL GOUTI^a, T. AIT TALEB^a

^aLaboratory of Condensed Matter Physics and Nanomaterials for Renewable Energy, Faculty of Sciences; University Ibn Zohr, Agadir, Morocco

^bLaboratory of Optoelectronics, Universitat Politècnica de València, Spain.

^cDepartment of chemistry, M.D.University, Rohtak, India

We report here the effect of temperature in bands structure performed in the envelope function formalism, effective mass and magneto- transport properties of n-type HgTe ($d_1=8.6$ nm) /CdTe ($d_2=3.2$ nm) superlattices (SLs). When d_2 increase the gap $E_g(\Gamma)$ decrease to zero, at the transition semiconductor to semimetal conductivity, and become negative accusing a semimetallic conduction after the point $T'(d_2T', ET')$. d_2T' and ET' increases with temperature and removes the transition to higher d_2 . $E_g(\Gamma)$ increases from 48 meV at 4.2 K to 105 meV at 300K. The Fermi level is constant ($E_F(2D) \approx 90$ meV) until 77K and increases to 167 meV at 300K. Our Theoretical calculations have provided good agreement with the experimental data. The formalism used here predicts that the system is semiconductor for our ratio $d_1/d_2 = 2.69$, when $d_2 < 100$ nm. In our case, $d_2=3.2$ nm and $E_g(\Gamma, 77K) = 60$ meV so this sample is a two-dimensional far-infrared detector semiconductor ($12 \mu\text{m} < \lambda_c < 28 \mu\text{m}$).

(Received September 28, 2013; accepted November 7, 2013)

Keywords: Superlattice HgTe / CdTe, Band structure, Magneto-transport properties, Effective mass, envelope function formalism, Hall effect, Shubnikov-de Haas effect, Far infrared detector.

1. Introduction

After several decades of research, technology analysis of infrared is widely recognized and used in the most advanced sectors of security, the police and the military. The work of Esaki and Tsu [1] caused a big interest to the study of superlattices made from alternating layers of two semiconductors. The development of molecular beam epitaxy (MBE) has allowed the fabrication different alloys, quantum wells and superlattices and the observation of a number of fine aspects present in optical and transport properties of these structures. Among them, III-V superlattices ($\text{Ga}_{1-x}\text{Al}_x\text{As-GaAs}$ [1-2]-type I), III-V (InAs/GaSb [3] - type II) and later II-VI superlattice (HgTe/CdTe [4] - type III). The later has been predicted as a stable alternative for application in infrared optoelectronic devices than the $\text{Hg}_{1-x}\text{Cd}_x\text{Te}$ alloys. Especially in the region of second atmospheric window (around 10 μm) which is of great interest for communication. Infrared detectors have sensing principle as the photovoltaic.

HgTe-CdTe superlattice has the advantage of an almost perfect lattice matching between the two compounds ($a = 0.648$ nm for CdTe against $a = 0.646$ nm HgTe). The lattice-matching within 0.3 % yield to a small interdiffusion between HgTe and CdTe layers at low temperature near 200°C by MBE. HgTe is a zero gap semiconductor [5] when it is sandwiched between the wide

gap semiconductor CdTe (1.6 eV at 4.2 K) layers to yield to a small gap HgTe/CdTe superlattice which is the key of an infrared detector.

A number of papers have been published devoted to the band structure of this system [4,6] as well as its magneto optical and transport properties [6]. In this paper we report effect of temperature in bands structure, effective mass and correlation with magneto- transport properties in a nanostructure far-infrared detector HgTe/CdTe superlattice.

2. Experimental Techniques

Our sample HgTe/CdTe superlattice was grown by molecular beam epitaxy (MBE) on a [111] CdTe substrate at 180 °C. The sample (124 layers) had a period $d=d_1+d_2$ where $d_1(\text{HgTe})=8.6$ nm and $d_2(\text{CdTe})= 3.2$ nm. It was cut from the epitaxial wafer with a typical sizes of $5 \times 1 \times 1 \text{mm}^3$. The ohmic contacts were obtained by chemical deposition of gold from a solution of tetrachloroauric acid in methanol after a proper masking to form the Hall crossbar. Carriers transport properties were studied in the temperature range 1.5-300K in magnetic field up to 17 Tesla. Conductivity, Hall Effect, and angular dependence of the transverse magnetoresistance were measured. The measurements at weak magnetic fields (up to 1.2 T) were performed into standard cryostat equipment. The

measurements of the magnetoresistance were done under a higher magnetic field (up to 17 T), the samples were immersed in a liquid helium bath, in the centre of a superconducting coil. Rotating samples with respect to the magnetic field direction allowed one to study the angular dependence of the magnetoresistance.

3. Theory results of structural bands

Calculations of the spectra of energy $E(d_2)$, $E(k_z)$ and $E(k_p)$, respectively, in the direction of growth and in plane of the superlattice; were performed in the envelope function formalism [4,6,8] with a valence band offset Λ between heavy holes bands edges of HgTe and CdTe of 40 meV determined by the magneto-optical absorption experiments [7].

The energy E as a function of d_2 , at $T=4.2$ K, 77 K and 300 K, in the centre Γ of the first Brillouin zone and for $d_1 = 2.68 d_2$, are shown in Fig.1. The case of our sample ($d_2 = 32 \text{ \AA}$) is indicated by the vertical solid line.

Here the cross-over of E_1 and HH_1 subbands occurs. d_2 controls the superlattice band gap $E_g = E_1 - HH_1$. For weak d_2 the sample is semiconductor with a strong coupling between the HgTe wells. For example, at $T = 4.2$ K as can be seen in Fig. 2 (a), at the point Γ ($d_{2T} = 100 \text{ \AA}$, $E_T = 38 \text{ meV}$) the gap goes to zero with the transition semiconductor- semimetal. From Fig. 2 we extracted the coordinates of the transition point T (d_{2T} , E_T). As seen in Fig. 3. d_{2T} and E_T increases with temperature. So the increase of the temperature removes the transition to higher d_2 .

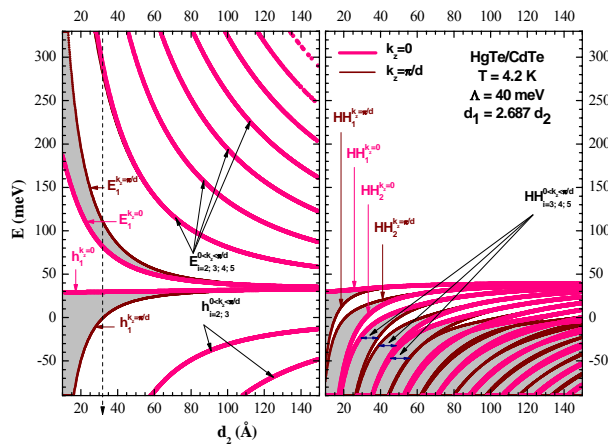


Fig 1. Energy position and width of the conduction (E_i), heavy-hole (HH), and the light-hole (h_l) subbands calculated at 4.2 K in the center Γ ($k_z=0$) and the limit ($k_z=\pi/d$) of the first Brillouin zone as a function of layer thickness d_2 for HgTe/CdTe superlattice with $d_1=2.687 d_2$, where d_1 and d_2 are the thicknesses of the HgTe and CdTe layers, respectively. $d_2=3.2 \text{ nm}$ of our sample is indicated by the vertical dashed line.

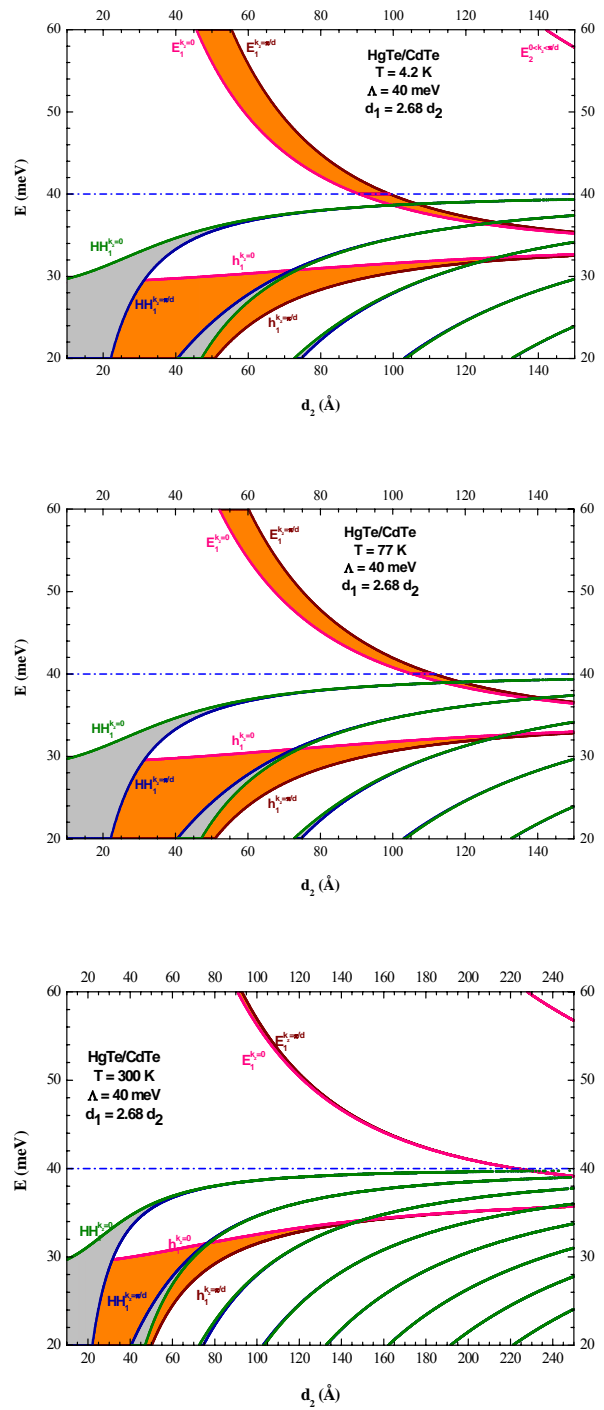


Fig. 2. Energy subband, calculated at 4.2 K, 77 K and 300 K in the center Γ ($k_z=0$) and the limit ($k_z=\pi/d$) of the first Brillouin zone, as a function of layer thickness d_2 for HgTe/CdTe superlattice with $d_1=2.68 d_2$, where d_1 and d_2 are the thicknesses of the HgTe and CdTe layers, respectively.

When d_2 increases, E_1 and h_1 states drops in the energy gap $[0, \Lambda]$ and become interface state with energy $E_1 = \Lambda \varepsilon_2 / (\varepsilon_1 + \varepsilon_2) = 34$ meV for infinite d_2 [8]. Then the superlattice has the tendency to become a layer group of isolated HgTe wells and thus assumes a semimetallic character. Note that we had observed a semimetallic conduction mechanism in the quasi 2D p type HgTe/CdTe superlattice [9].

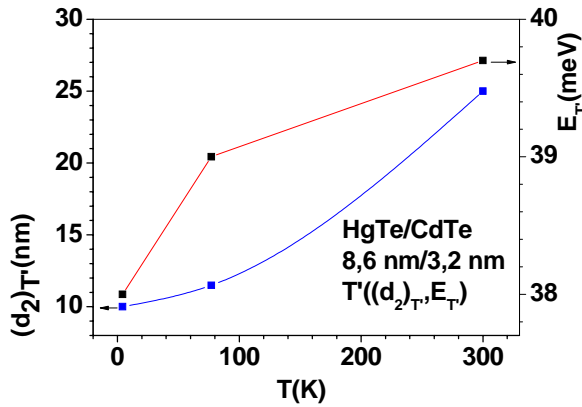


Fig. 3. Temperature dependence of the coordinates of the transition point $T'(d_{2T}, E_T)$ at the center Γ of the first Brillouin zone of the HgTe/CdTe superlattice.

In the left of Fig 2, we can see that the band gap E_g increase when d_2 decrease and the temperature increase. From Fig. 2 and for our $d_2 = 3.2$ nm we get the temperature dependence of the band gap E_g , in the centre Γ of the first Brillouin zone in Fig.4. Note that E_g increases from 48 meV at 4.2 K to 105 meV at 300K.

We calculated the detection cut-off wave length by the relation:

$$\lambda_c(\mu\text{m}) = 1240/E_g(\text{meV}). \quad (1)$$

In the investigated temperature range $12 \mu\text{m} < \lambda_c < 28 \mu\text{m}$ situates our sample as a far infrared detector.

For an anisotropic medium, such as the HgTe/CdTe superlattices, the effective mass is a tensor and its elements along μ and ν directions are given by the following expression [10]:

$$\left(\frac{1}{m^*}\right)_{\mu\nu} = \frac{1}{\hbar^2} \frac{\partial^2 E_{k_{\mu\nu}}}{\partial k_{\mu} \partial k_{\nu}} \quad (2)$$

By carrying out second derivative of the energy E_1 , h_1 and HH_1 along k_z and k_p , from the spectres of energy $E(k_z)$ and $E(k_p)$, respectively, in the direction of growth and in plane of the superlattice at different temperatures (in Fig. 5 for example), we calculated the effective mass bands in Fig. 6. For example at $T = 4.2$ K, along k_p , the effective mass of heavy holes is $m_{HH1}^* = -0.30 m_0$ and the effective

mass of electrons m_{E1}^* increases from $0.04 m_0$ to $0.11 m_0$. In Fig.4 (a), the Fermi level across the conduction band E_1 at $k_p = 0.01 \text{ \AA}^{-1}$ corresponding to $m_{E1}^*(E_F) = 0.05 m_0$. Whereas, the effective mass of the light holes h_1 decreases from $0.24 m_0$, to a minimum of $(m_{h1}^*)_{\min} = 0.16 m_0$ at $k_p = 0.01 \text{ \AA}^{-1}$, and increase to $0.30 m_0$ assuming an electronic conduction. Along K_z , m_{E1}^* increase and diverge at 0.011 \AA^{-1} , 0.015 \AA^{-1} and 0.022 \AA^{-1} respectively.

After it increase to 0 assuming a hole conduction. The comportment of m_{E1}^* and m_{HH1}^* are inverse to that of m_{E1}^* discussed above. In all temperature range, $m_{HH1}^* = -0.30 m_0$ and the Fermi level $E_F = 88$ meV across the conduction band E_1 at $k_p = 0.01 \text{ \AA}^{-1}$ corresponding to $m_{E1}^*(E_F) = 0.05 m_0$.

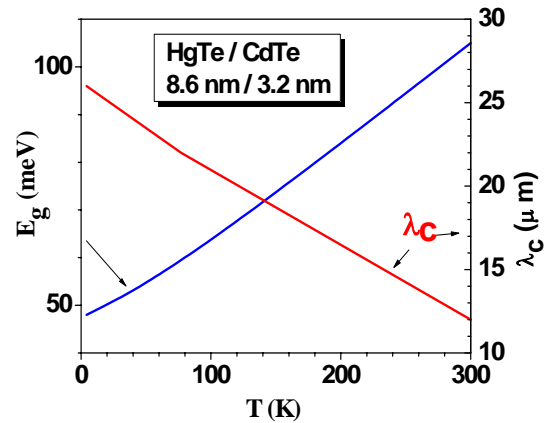


Fig. 4. Temperature dependence of the band gap E_g and the cut-off wavelength λ_c , at the center Γ of the first Brillouin zone.

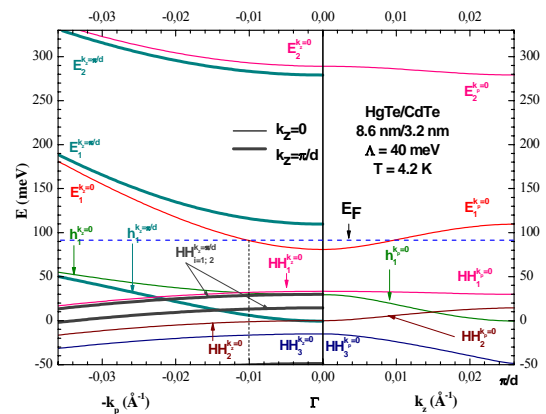


Fig. 5. Calculated bands along the wave vector k_z and in plane $k_p(k_x, k_y)$ at 4.2 K.

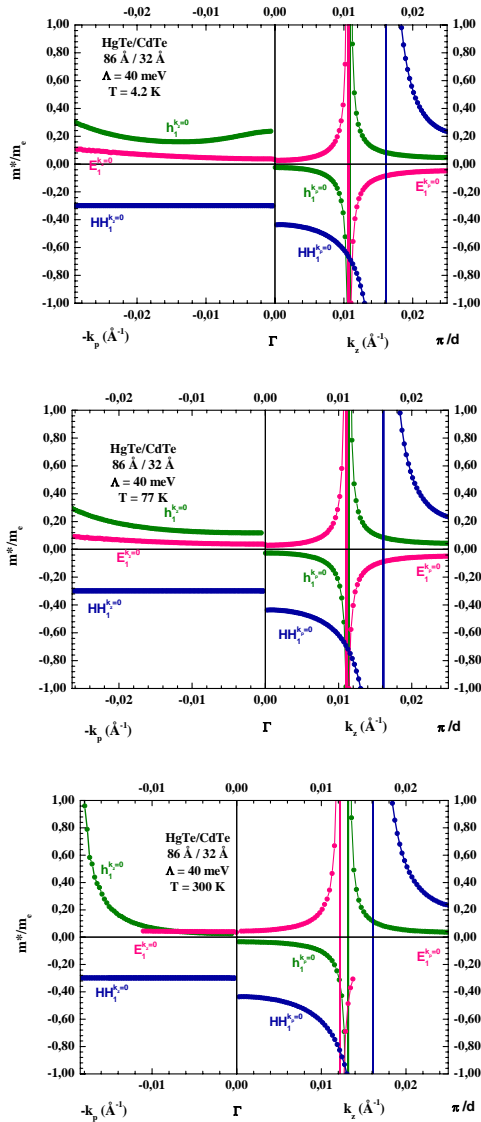


Fig. 6. Calculated relative effective mass bands along the wave vector k_z and in plane k_p of the HgTe/CdTe superlattice at 4.2 K, 77 K and 300 K.

4. Experimental results and discussions

The variation of the magnetoresistance ΔR disappears as the magnetic field is parallel to the plane of the superlattice indicating a two dimensional (2D) behaviour supported by the observation of Shubnikov-de Haas effect oscillations in Fig. 7.

We have also measured the conductivity and Hall mobility. At low temperatures, the sample exhibits n type conductivity $\sigma_0 = 0.011 \Omega^{-1}$ in Fig. 8(a) with a concentration $n = 1/e |R_H| = 3.24 \times 10^{12} \text{ cm}^{-2}$ from Fig. 8(b) and a Hall mobility $\mu_H = 2.5 \times 10^5 \text{ cm}^2/\text{Vs}$ in Fig. 8(c). The plot $\log(\mu_n) - \log(T)$ of the Hall mobility shows a scattering of electrons by phonons in the intrinsic regime with

$\mu_H \sim T^{1.58}$ and weak activation energy at low temperature with $\mu_H \sim T^{0.05}$ [11].

This relatively high mobility allowed us to observe the Shubnikov-de Haas effect until 8 Tesla. Its well known that the oscillations of the magnetoresistance are periodic with respect to $1/B$. The period $\Delta(1/B)$ is related to the concentration n of the electrons by the relation [5]:

$$n = e / \pi h \Delta(1/B) \quad (3)$$

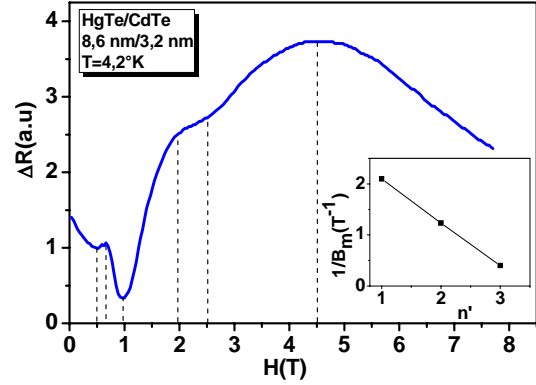


Fig. 7. Variation of the transverse magneto-resistance, with magnetic field at 4.2 K, in the investigated HgTe/CdTe superlattice.

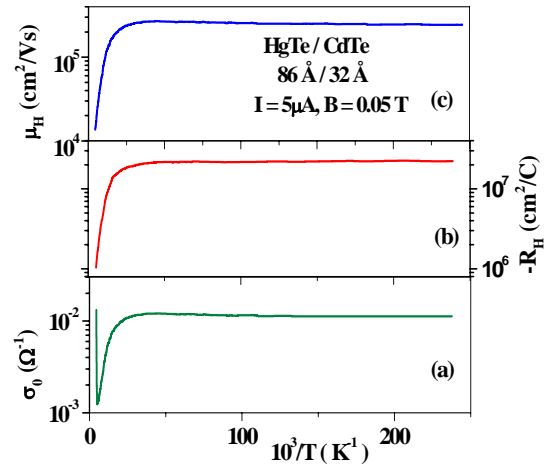


Fig. 8. Temperature dependence of the Hall mobility (c), weak-field Hall coefficient (b) and conductivity (a) in the investigated HgTe/CdTe superlattice.

In the insert of Fig. 8 we have plot the inverse of the minima's $1/B_m$ as a function of the entire n' following the formula:

$$1/B_m = \Delta(1/B)(n'+1/2) \quad (4)$$

The linear line slope gives $\Delta(1/B)$ and $n = 3.20 \times 10^{12} \text{ cm}^{-2}$ in good agreement with that measured by weak field Hall effect ($B=0.5 \text{ KOe}$, $I=5 \mu\text{A}$) from Fig. 8(b).

At low temperature, the superlattice electrons dominate the conduction in plane. The E_1 band is not parabolic with respect to k_p^2 . That permits us to estimate the Fermi energy (2D) $E_F = n\pi\hbar^2 / (m_{E_1}^*)_{E_F} = 88 \text{ meV}$. Fig. 9 show that the Fermi level is constant ($E_F(2D) \approx 90 \text{ meV}$) until 77K and increases to 167 meV at 300K.

This HgTe/CdTe superlattice is a stable alternative for application in far infrared optoelectronic devices than the random alloys $\text{Hg}_{0.99}\text{Cd}_{0.01}\text{Te}$ because the small composition $x=0.01$, with $E_g(\Gamma, 300 \text{ K})=100 \text{ meV}$ given by the empiric formula for $\text{Hg}_{1-x}\text{Cd}_x\text{Te}$ [12] is difficult to obtain with precision while growing the ternary alloys and the transverse effective masse in superlattice is two orders higher than in the alloy. Thus the tunnel length is small in the superlattice.

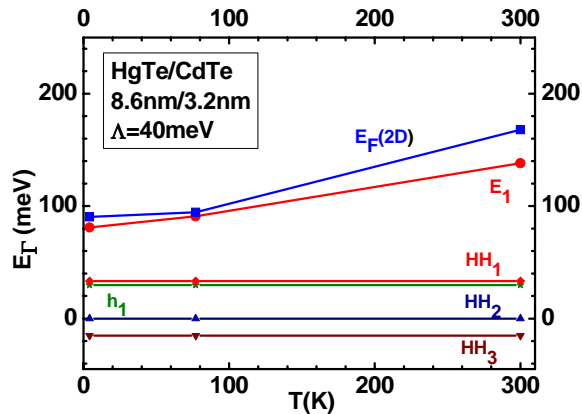


Fig. 9. Variation of the Energy subbands and Fermi level E_F , at the center Γ of the first Brillouin zone, as a function of temperature in the investigated HgTe/CdTe superlattice.

5. Conclusions

We reported here electronic properties of a two-dimensional superlattice nanostructure. The formalism used here predicts that the system is semiconductor, for our HgTe to CdTe thickness ratio $d_1/d_2 = 2.69$, when $d_2 < 100 \text{ nm}$. In our case, $d_2=3.2 \text{ nm}$ and $E_g(\Gamma, 4.2 \text{ K}) = 48 \text{ meV}$. In spite of it, the sample exhibits the features typical for the semiconductor type n conduction mechanism. In

the used temperature range, this sample is a far-infrared detector, narrow gap and two-dimensional n-type semiconductor. The theoretical and magneto transport parameters are in good agreement. In conclusion, the HgTe/CdTe superlattice is a stable alternative for application in infrared optoelectronic devices than the alloys $\text{Hg}_{1-x}\text{Cd}_x\text{Te}$. Measurements performed by us on others' samples indicate an improvement of quality of the material manifested by higher mobility.

References

- [1] L. Esaki, R. Tsu, IBM J. Res. Dev. 61–65 (1970)
- [2] R. Dingle, A.C. Gossard, W. Wiegmann, Phys. Rev. Lett. **34**, 1327 (1975)
- [3] H. Sakaki, L.L. Chang, G.A. Sai-Halasz, C.A. Chang, L. Esaki, Solid State Commun. **26**(9), 589 (1978)
- [4] G. Bastard, Phys. Rev. B **25**, 7584 (1982)
- [5] J. Tuchendler, M. Grynberg, Y. Couder, H. Thomé, R. Le Toullec, Phys. Rev. B **8**, 3884 (1973)
- [6] Ab. Nafidi, et al, in Book of Abstracts of the International Conference on Theoretical Physics (HT 2002), Paris, France, 22–27 July (2002), pp. 274–275
- [7] N.F. Johnson, P.M. Hui, H. Ehrenreich, Phys. Rev. Lett. **61**, 1993 (1988)
- [8] A. El Abidi, A. Nafidi, H. Chaib, A. El Kaaouachi, M. Braigue, R. Morghi, E.Y. EL Yakoubi, M. d'Astuto, Physica B: Physics of Condensed Matter **405**, 936 (2010).
- [9] A. Nafidi, "Band Structure and Magneto-Transport Properties in II-VI Nanostructures Semiconductors-Application to Infrared Detector Superlattices," in Optoelectronic Devices and Properties, edited by Oleg Sergiyenko, Rijeka: INTECH, 2011, pp. 283-304
- [10] C. Kittel, Introduction to Solid State Physics, 3rd edn. (Wiley, New York, 2001), p. 333
- [11] M. Braigue, A. Nafidi, H. Chaib, Devki N. Talwar, A. Tirbiyine et al., AIP Conf. Proc. **1416**, 68 (2011); doi: 10.1063/1.3671700
- [12] G.L. Hansen, J.L. Schmit, T.N. Casselman, J. Appl. Phys. **53**, 7099 (1982)

*Corresponding authors: nafidi21@yahoo.fr